WORLD JOURNAL OF PHARMACY AND PHARMACEUTICAL SCIENCES
SJIF Impact Factor 7.632
Volume 9, Issue 7, 251-277 Research Article ISSN 2278 – 4357

QUALITY BY DESIGN: A SYSTEMATIC APPROACH USING AN ADVANCED STATISTICAL TOOL TO OPTIMIZATION OF NIOSOMES PREPARATION FOR THE TOPICAL DELIVERY

Parinbhai Shah[1,2], Benjamin Goodyear[1,2], Anika Haq[1,2], Vinam Puri[1,2] and Bozena Michniak-Kohn*[1,2]

[1]Department of Pharmaceutics, Ernest Mario School of Pharmacy, Rutgers, The State University of New Jersey, Piscataway.

[2]Center for Dermal Research, Life Science Building, Rutgers, The State University of New Jersey, Piscataway.

Article Received on
26 April 2020,

Revised on 16 May 2020,
Accepted on 06 June 2020

DOI: 10.20959/wjpps20207-16485

***Corresponding Author**
Bozena Michniak-Kohn
Department of Pharmaceutics, Ernest Mario School of Pharmacy, Rutgers, The State University of New Jersey, Piscataway.
michniak@pharmacy.rutgers.edu

ABSTRACT

QbD is a systematic approach that may be used to improve product quality, process understanding, and supporting adequate regulatory compliance for vehicle-based drug delivery systems commonly used in the pharmaceutical industry. The purpose of this investigation was to optimize critical material attributes & critical process parameters to effectively develop a niosomal drug delivery system for use with the topical application of desoximetasone. Formulation variables considered were based on previous research of niosome CMAs (surfactant & cholesterol concentrations), and CPPs (mixing time, mixing speed, & organic phase addition rate) variables. An extensive 2^5 factorial design was created using JMP® statistical software better to understand the effects of these parameters on niosome formulations. Experiments were systematically conducted to develop an in-silico profile predictor using the fit model and 3D surface plots. Various profile predictions were generated, and best fit model regression lines were selected to validate the niosome QTPP. An optimized formulation with 450 nm particle size and a 90% entrapment efficiency was obtained using a drug, surfactant, and cholesterol ratio (1:2:1) with an external phase temperature of 65°C, internal and external phase volume of 10 and 20 mL respectively, mixing parameters 650 rpm and 50 minutes and addition rate of 0.5 mL/min. By selecting specified CMAs and CPPs, optimized niosome vesicles containing desoximetasone was achieved successfully.

KEYWORDS: Quality by Design (QbD), JMP® statistical software, Critical Material Attributes and Critical Process Parameters, Desoximetasone, Controlled drug delivery, Niosome, Allergic reactions, Topical drug delivery, Psoriasis, Eczema.

GRAPHICAL ABSTRACT

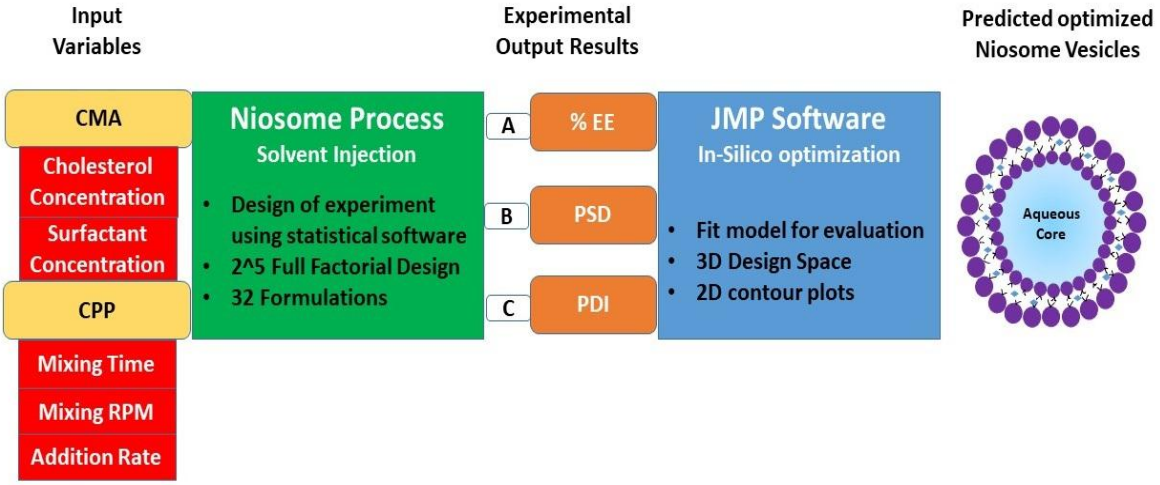

1. INTRODUCTION

Topical dosage forms are commonly used to produce a localized therapeutic effect at the site of administration onto the skin.[1,2] Formulations for skin delivery are effectively developed using commonly used drug delivery vehicles across the pharmaceutical industry to treat patients with various disease states.[3] Atopic dermatitis (AD) is an itchy, chronic inflammatory skin disease with frequently remitting and relapsing symptoms.[4] Treating chronic disease forces patients to seek various topical remedies classified as modern day emollients.[5] In the early 1950s, topical drug delivery emerged in the topical corticosteroids marketplace when medical doctors successfully treated skin conditions using steroid therapy.[6,7]

Today, psoriasis and eczema are some of the most commonly diagnosed skin conditions. Psoriasis is an autoimmune skin condition where the skin cells multiply up to 10 times faster than usual. As a consequence, the top layer of the epidermis appears as thick, red, and white hues of scaly patches that are itchy, dry and may give rise to swelling, pain, and tiresome disease.[8,9] Study results from topical corticosteroid formulation, such as fluticasone propionate and mometasone furoate revealed that daily one dosing led to less systemic absorption and showed identical efficacy when compared to daily twice dosing.[10,11] In this case, reduced frequency of dose not only improved compliance but also reduced the side

effects.[12] Topical corticosteroids are the mainstay for atopic dermatitis therapy[13] and have shown positive results in several other treatments such as atrophy, perioral dermatitis, acne, and rosacea.[14] Desoximetasone (DM) is one such topical corticosteroid that is effective, safe and well tolerated by patients.[15] It has been made available in the form of creams and ointments.[16-18] However, there are no formulations currently that can release DM over an extended period of time.

Non-ionic surfactant-based vesicles – niosomes are nanocarriers composed of non-ionic surfactants and cholesterol, which demonstrate safe and effective targeted drug delivery.[19,20] The formation of vesicular structures by amphiphilic surfactants occurs spontaneously in aqueous media upon applying energy, resulting in a closed bilayer structure with the hydrophobic portion forming the inner portion and the hydrophilic part facing outwards.[20] Although niosomes were first used in cosmetics,[21] their application was soon adopted for drug delivery[22] because of their potential to offer targeted drug delivery. Several factors exist during the formation of niosomes such as- type of surfactant, nature of the encapsulated drug, charge of the particle, and the processes of synthesizing that affect their properties and stability.[23] The therapeutic efficacy of the drug loaded in the niosomal matrix can be improved by reducing the clearance rate, targeting the desired site, and by protecting the encapsulated drug.[24]

The commonly used Traditional one-factor-at-a-time (OFAT) experimental design has many drawbacks that require an arduous amount of time and resources to conduct a robust formulation design adequately.[25] When more scientific resources are available, the Design of Experiments (DoE) is a more logical approach to multivariate statistics that aim to guide the scientific investigation to study the effects of multiple factors simultaneously, not only individually, but also on their interactions.[26] A full-factorial experimental study design enables researchers to systematically study the responses of different factors, relations between factors and interactions between factors by effectively quantifying scientific error.[27] JMP® by SAS institute is a statistical tool that may be used to select best-fit during computational modeling to ascertain a detailed understanding of the results obtained using a Quality by Design (QbD) approach,[28,29]

Over the years, the pharmaceutical industry has spent significant efforts to ensure product quality, to achieve regulatory compliance, and to yield pharmaceuticals as cost-efficient as

possible. Therefore, advanced processes and technologies that require steadiness among operational complexity and scientific progress are being applied.[30] QbD is a new advanced systematic risk-based approach applied to pharmaceuticals to develop formulations with predefined objectives and intensify product and process understanding with improved safety and stability.[31] Application of the QbD approach is believed to have a significant impact on pharmaceutical quality regulation as opposed to older empirical processes that pose a higher risk of failure or suboptimal quality.[32,33]

US Food and Drug Administration (FDA) is requesting pharmaceutical companies to adopt risk-based approaches and QbD principles in product development from research and development through the manufacturing cycle.[34] Pharmaceutical QbD has expanded with the issuance of ICH Q8 (R2) (Pharmaceutical Development), ICH Q9 (Quality Risk Management), and ICH Q10 (Pharmaceutical Quality System).[35-37] This makes it a highly demanded process to avoid product failure during manufacturing and to achieve regulatory requirements.

The present work is aimed at utilizing a JMP®-enabled DoE approach to formulate desoximetasone loaded niosomes. As per the principles of QbD, the methodology started with setting the Quality Target Product Profile (QTPP) and identifying the Critical Quality Attributes (CQAs) needed to meet that. The Critical Process Parameters (CPPs) and Critical Material Attributes (CMAs) were evaluated to identify their impact on the CQAs. DOE is used in this study for risk evaluation and optimization and to understand the effects of different variables on the responses. Experimental trials were defined by using full factorial designs for achieving the optimized formulation, and the process was finally validated and tested for robustness.

2. MATERIALS AND METHODS

2.1. Materials

Desoximetasone was gifted by Flavine, New Jersey, USA. HPLC Water, Diethyl ether, Stearylamine, and Chloroform were procured from Sigma-Aldrich, Saint Louis, MO, USA. Methanol, Acetone, and Acetonitrile were obtained from BDH VWR Analytical, Radnor, PA, USA. Ethanol was purchased from Decon Labs, Inc., King of Prussia, PA, USA. Span 60 and Cholesterol were gifted from Croda Inc., Mill Hall, PA, USA. Stearic Acid was a gift from BASF Corporation, Edison, NJ, USA. Glacial Acetic Acid was purchased from Fisher Scientific, Fair Lawn, NJ, USA.

2.2. Niosome vesicle preparation

The niosomes were prepared by ether injection method with the drug dissolved into the 10 mL organic phase diethyl ether: methanol (75:25) until completely dissolved. Next, sorbitan monostearate (Span 60), cholesterol, and stearic acid added into the mixture and mixed using a suitable magnetic stir bar in a 20 mL glass scintillation vial. In a separate 50 mL glass beaker, 20 mL purified water was preheated at 65°C temperature as per the batch design using a hot plate with magnetic stirring. The organic phase was filled into a 10 mL syringe with a 26 G needle. The organic phase mixture was injected into the preheated aqueous phase using prefixed parameters based on the experimental study design. Mixing was continued based on the values identified from the design of experiment (DOE). In the final step of the process, the batch formulation was cooled down to room temperature, and the formulation was stored in a suitable glass storage container.

2.3. HPLC method

The mobile phase was prepared by combining methanol, HPLC grade water, and glacial acetic acid (65:35:1). Diluent was prepared using methanol and acetonitrile (50:50). Desoximetasone concentrations were measured using a Discovery C18 column of 150 mm x 4.6 mm with 5 µm particle size, with UV detector absorbance set to 254 nm. The injection volume was 10 µL, and the flow rate was 1.0 mL/min. The sample run time was 10 minutes at room temperature, and retention time for the drug elution peak was at approximately 5 min. The linearity measurements were performed as per the ICH guideline with six serial dilutions range from 0.0025 to 0.08 mg/mL with an R^2 value of 0.999.

2.4. Optimization of desoximetasone loaded niosomes by DOE

The present study was conducted utilizing QbD approach to formulate the desoximetasone loaded niosomes and understand the impact of each formulation variables.

2.4.1. Identifying CMAs and CPPs

Parameters were identified for testing based on our prior knowledge about vesicular drug delivery systems combined with an extensive literature review of patents, scientific peer review journals, expert opinions, and research articles. Selected parameters for investigation were an organic phase, drug concentration, surfactant concentration, cholesterol concentration, and types of lipids as CMAs and internal and external phase volumes, external phase temperature, mixing time, mixing speed, and addition rate as the CPPs. Preliminary experiments defined that Diethyl ether: Methanol (75: 25), 20 mg Desoximetasone, 65°C

external phase temperature, 20 mL external phase volume, and 10 mL internal phase volume were acceptable ranges to form noisome formulations spontaneously.[38] Both independent and dependent variables selected are described in Table 1 define each low and high associated use levels.

Table 1: CMAs and CPPs for the design of formulation.

Variables	Levels	
	-1	+1
Independent variables		
X_1 = Span 60 (mg)	40	60
X_2 = Cholesterol (mg)	20	40
X_3 = Mixing Speed (RPM)	450	650
X_4 = Mixing Time (Minutes)	45	60
X_5 = Addition Rate (mL/min)	0.5	1
Dependent variables		
Y_1 = Particle Size (nm)		
Y_2 = Entrapment Efficiency (%)		
Y_3 = Polydispersity Index		

Batches were formulated using a 2^5 randomized full factorial design (Table 2), and the effect of surfactant concentration (X_1), cholesterol concentration (X_2), mixing speed (X_3), mixing time (X_4) and addition rate (X_5) were considered to be independent variables. The dependent variables measured were entrapment efficiency (Y_1), particle size (Y_2), and polydispersity index (Y_3). The factors were studied at two levels (-1, +1) as described in Table 2, and symbols in the pattern column represent their combinations. The factorial experimental design was developed using JMP® statistical software from SAS, and the responses found were input back to the software. The best fit model was selected based on results from previous experimental data and using the response profile predictor by JMP®.[38] These tools help to formulate with relatively better accuracy using mathematical modeling.

Table 2: Full factorial design guiding the formulation of niosomal dispersion batches obtained using the QbD approach.

Batch Detail	Pattern	Span 60	Cholesterol	Mixing Speed	Mixing Time	Addition Rate
		X_1	X_2	X_3	X_4	X_5
DND-30	+ − − + −	+1	-1	-1	+1	-1
DND-31	− − + − +	-1	-1	+1	-1	+1
DND-32	+ + + − −	+1	+1	+1	-1	-1
DND-33	− + + − +	-1	+1	+1	-1	+1
DND-34	+ − − + +	+1	-1	-1	+1	+1
DND-35	− − − + +	-1	-1	-1	+1	+1
DND-36	− + − + −	-1	+1	-1	+1	-1
DND-37	+ − + − +	+1	-1	+1	-1	+1
DND-38	− + − − +	-1	+1	-1	-1	+1
DND-39	− − − − −	-1	-1	-1	-1	-1
DND-40	− + − + +	-1	+1	-1	+1	+1
DND-41	+ + − − +	+1	+1	-1	-1	+1
DND-42	+ + + − +	+1	+1	+1	-1	+1
DND-43	+ − + − −	+1	-1	+1	-1	-1
DND-44	− − + + +	-1	-1	+1	+1	+1
DND-45	− − − − +	-1	-1	-1	-1	+1
DND-46	+ − − − +	+1	-1	-1	-1	+1
DND-47	− − − + −	-1	-1	-1	+1	-1
DND-48	+ + − + −	+1	+1	-1	+1	-1
DND-49	− + + − −	-1	+1	+1	-1	-1
DND-50	+ + − − −	+1	+1	-1	-1	-1
DND-51	+ − − − −	+1	-1	-1	-1	-1
DND-52	+ + + + −	+1	+1	+1	+1	-1
DND-53	− − + + −	-1	-1	+1	+1	-1
DND-54	+ + − + +	+1	+1	-1	+1	+1
DND-55	+ − + + −	+1	-1	+1	+1	-1
DND-56	− + + + +	-1	+1	+1	+1	+1
DND-57	− + − − −	-1	+1	-1	-1	-1
DND-58	+ + + + +	+1	+1	+1	+1	+1
DND-59	− − + − −	-1	-1	+1	-1	-1
DND-60	+ − + + +	+1	-1	+1	+1	+1
DND-61	− + + + −	-1	+1	+1	+1	-1

2.5. Niosome vesicle characterization

2.5.1. Organoleptic properties

Niosomal dispersions were characterized for visual appearance, color, and odor to confirm the presence of any residual solvent as a standard quality check.

2.5.2. Drug content (assay determination)

The desoximetasone niosomal dispersion 100 mg was carefully collected and placed into an intermediate solvent containing a chloroform: methanol (40:60) mixture and then mixed using vortex until it was dissolved entirely at room temperature. Upon mixing, niosomal dispersion samples were further diluted with an equal ratio of diluent. Drug content quantification for desoximetasone was performed using HPLC coupled with UV analysis at a wavelength of λ_{max} 254 nm. The HPLC instrument used was Agilent 1100 series instrumentation (Agilent Technologies, CA, USA) coupled with UV detection (DAD) and HP ChemStation software V. 32.

2.5.3. Drug entrapment efficiency of niosome vesicles

The desoximetasone free drug was determined from entrapped drug by ultracentrifugation at set to 14,000 rpm for 30 min using an ultracentrifuge (Branson Ultrasonic Corporation, CT, USA) at room temperature (centrifuge speed was validated using 3750 rpm and 14,000 rpm and centrifugation time was validated using 30 min and 60 min). The supernatant containing the free available drug was carefully collected without disturbing the sediment, and 200 mg of the collected supernatant was dissolved into chloroform: methanol (40:60) mixture using a vortex mixer. After mixing, the sample was further diluted with an equal amount of the diluent. Drug quantification was determined using the predetermined HPLC method. Drug % entrapment efficiency was calculated in triplicate by using the following formula.[39]

$$\% \text{ Entrapment Efficiency} = \frac{Total\ amount\ of\ drug - Free\ amount\ of\ drug}{Total\ amount\ of\ drug} \times 100$$

2.5.4. Niosomes vesicle size and zeta potential

The mean vesicle size and its distribution were estimated at room temperature using a Delsa Nano S Particle Sizer (Beckman Coulter, CA, USA) in triplicate based on the light scattering spectroscopy principles. The zeta potential of the niosomal suspensions was measured in triplicate using a Malvern Particle Sizer 2000 (Malvern Technologies, Worcestershire, UK).

2.6 Validation of profile predictor by check point formulas

Formulation results were evaluated and entered in full factorial design from JMP®. Based on the available results, using the fit model profile predictor was generated. Two formulation combinations were generated using a profile predictor. Both batches were manufactured, and actual batch data were compared with model predicted data to verify profile predictor accuracy.

3. RESULTS AND DISCUSSION

Based on the observed experimental data, current study demonstrates the impact on the niosome formulations caused by the CPPs, surfactant concentrations, presence of membrane additives, and drug specific physicochemical attributes.

Surfactants containing an alkyl-chain length ranging from C12-C18 are typically preferred due to favorable skin compatibility.[40] The results from current study demonstrated that alkyl chain length was a key parameter suitable for effective drug encapsulation. Span 60 (sorbitan monostearate) was sufficient to be used as the primary surfactant in the preparation of niosomal vesicles due to the stability from longer saturated alkyl chains. Higher entrapment efficiency was achieved using longer chain lengths. The physicochemical properties associated with these findings may be linked to a higher phase transition temperature and lower HLB (4.7) of Span 60, which resulted in higher entrapment efficiency.[41]

CMAs & CPPs were considered to have the most substantial impact on the various performance aspects of niosomes containing desoximetasone. Various quantitative measurements were used to evaluate their impact on entrapment efficiency (%), particle size (nm), polydispersity index (PDI), and zeta potential (mV).

CMAs identified with the greatest potential to impact product quality aspects, were drug concentration, Span 60 concentration, cholesterol concentration and type of lipids. CPPs tested were external phase temperature (°C), external phase volume (mL), internal phase volume (mL), mixing time (minutes), mixing speed (rpm), and addition rate (mL/min).

3.1. Organoleptic properties

All the niosomal formulations obtained were characterized by their physical state as milky white, odorless dispersions with a fluid-like consistency.

3.2. Experimental design for optimizing niosomes

Niosome formulations were prepared following using the full-factorial design of the experiment to measure the associated effect of selected formulation variables. Variables measured were surfactant and cholesterol concentrations, total mixing time, mixing speed, and addition rate. Niosomal input variables were chosen with the assumption that their use levels are acceptable for a range of vehicle interactions.

Details regarding formulations tested using an acceptable range of low and high values (+1, -1) are defined using input variables (X_1, X_2, X_3, X_4, X_5) in Table 3 with associated dependent variables (Y_1, Y_2, Y_3, & Zeta Potential (mV)) measurements. (Entrapment efficiency, particle size, polydispersity index, and zeta potential). The entrapment efficiency was found to be varying between 83.68 - 93.72%, whereas particle size and polydispersity index were found to be in the ranges of 326.53 – 1730.83 nm and 0.285 – 0.422, respectively.

Table 3: DOE observed responses for desoximetasone loaded niosomes using a 2^5 full factorial design. (N = 3, mean ± SD).

Batch Detail	Design Input (Independent Variables)					Design Output (Dependent Variables)			
	X_1	X_2	X_3	X_4	X_5	Y_1	Y_2	Y_3	
	Span 60	Chole-sterol	Mixing Speed	Mixing Time	Addition Rate	Entrapment Efficiency (%)	Particle Size (nm)	Polydispersity Index	Zeta Potential (mV)
DND-30	+1	-1	-1	+1	-1	92.06 ± 0.03	1076.57 ± 13.94	0.400 ± 0.00	-73.63 ± 1.89
DND-31	-1	-1	+1	-1	+1	92.06 ± 0.04	411.90 ± 9.07	0.350 ± 0.01	-77.37 ± 1.60
DND-32	+1	+1	+1	-1	-1	90.65 ± 0.02	632.63 ± 16.98	0.354 ± 0.02	-70.57 ± 3.41
DND-33	-1	+1	+1	-1	+1	90.13 ± 0.05	487.73 ± 12.50	0.330 ± 0.00	-77.20 ± 0.62
DND-34	+1	-1	-1	+1	+1	90.58 ± 0.01	888.37 ± 61.11	0.350 ± 0.02	-39.27 ± 3.33
DND-35	-1	-1	-1	+1	+1	88.37 ± 0.15	598.00 ± 38.84	0.302 ± 0.01	-57.27 ± 3.87
DND-36	-1	+1	-1	+1	-1	92.28 ± 0.06	965.20 ± 27.51	0.358 ± 0.01	-68.43 ± 1.21
DND-37	+1	-1	+1	-1	+1	90.49 ± 0.03	645.30 ± 27.72	0.315 ± 0.03	-69.87 ± 1.27
DND-38	-1	+1	-1	-1	+1	90.23 ± 0.04	1730.83 ± 100.45	0.422 ± 0.05	-54.10 ± 0.44
DND-39	-1	-1	-1	-1	-1	90.71 ± 0.04	748.67 ± 8.75	0.302 ± 0.01	-54.80 ± 0.95
DND-40	-1	+1	-1	+1	+1	89.06 ± 0.02	821.13 ± 4.20	0.331 ± 0.02	-37.60 ± 3.75
DND-41	+1	+1	-1	-1	+1	87.99 ± 0.02	739.57 ± 31.08	0.360 ± 0.03	-61.67 ± 1.52
DND-42	+1	+1	+1	-1	+1	88.14 ± 0.05	564.13 ± 4.92	0.338 ± 0.01	-36.77 ± 1.12
DND-43	+1	-1	+1	-1	-1	91.48 ± 0.01	380.83 ± 7.49	0.312 ± 0.01	-51.70 ± 2.23
DND-44	-1	-1	+1	+1	+1	89.96 ± 0.03	476.33 ± 7.19	0.322 ± 0.03	-31.73 ± 1.05
DND-45	-1	-1	-1	-1	+1	91.37 ± 0.02	480.70 ± 10.57	0.310 ± 0.01	-53.17 ± 0.40
DND-46	+1	-1	-1	-1	+1	83.68 ± 0.04	548.10 ± 18.71	0.298 ± 0.03	-57.63 ± 1.31
DND-47	-1	-1	-1	+1	-1	93.72 ± 0.01	678.43 ± 14.00	0.344 ± 0.01	-57.93 ± 2.08
DND-48	+1	+1	-1	+1	-1	91.34 ± 0.01	974.07 ± 52.01	0.383 ± 0.01	-45.27 ± 0.86
DND-49	-1	+1	+1	-1	-1	92.71 ± 0.06	912.47 ± 32.65	0.360 ± 0.01	-56.47 ± 1.11
DND-50	+1	+1	-1	-1	-1	89.87 ± 0.07	664.27 ± 7.72	0.356 ± 0.01	-70.60 ± 0.35
DND-51	+1	-1	-1	-1	-1	86.80 ± 0.01	621.93 ± 25.32	0.285 ± 0.02	-70.80 ± 0.17
DND-52	+1	+1	+1	+1	-1	91.77 ± 0.06	370.33 ± 7.70	0.326 ± 0.01	-76.70 ± 2.86
DND-53	-1	-1	+1	+1	-1	90.55 ± 0.04	492.23 ± 23.32	0.294 ± 0.03	-44.43 ± 1.72
DND-54	+1	+1	-1	+1	+1	90.42 ± 0.07	457.83 ± 20.34	0.298 ± 0.01	-43.43 ± 1.46
DND-55	+1	-1	+1	+1	-1	89.39 ± 0.01	765.73 ± 29.57	0.316 ± 0.01	-49.17 ± 1.69
DND-56	-1	+1	+1	+1	+1	89.11 ± 0.08	712.27 ± 6.35	0.350 ± 0.02	-47.27 ± 2.40
DND-57	-1	+1	-1	-1	-1	90.72 ± 0.04	750.00 ± 37.12	0.345 ± 0.02	-60.03 ± 2.50
DND-58	+1	+1	+1	+1	+1	91.01 ± 0.02	413.83 ± 12.60	0.326 ± 0.01	-63.00 ± 1.32
DND-59	-1	-1	+1	-1	-1	89.15 ± 0.05	552.63 ± 33.04	0.302 ± 0.02	-47.40 ± 2.00
DND-60	+1	-1	+1	+1	+1	87.29 ± 0.05	326.53 ± 8.13	0.303 ± 0.00	-47.67 ± 0.91
DND-61	-1	+1	+1	+1	-1	90.75 ± 0.02	599.93 ± 14.02	0.344 ± 0.01	-70.40 ± 0.95

3.3. Analysis of responses

Responses observed from 32 formulations using JMP® were used for evaluating potential significant differences using full-factorial design methodologies.

3.3.1. Response 1 (Y_1): effect of formulation variables on entrapment efficiency

Vesicular entrapment efficiency is commonly linked to the stability of noisome vesicles. Various parameter combinations to manufacture a niosome dispersion were summarized in

the design Table 3 associated Y_1 results. A "best-fit" model approach was suitable to analyze further the R^2 value shown in Table 4 along with the regression equation without requiring further data transformation method. CMAs & CPPs both had a significant impact on niosome entrapment efficiency.

Using an appropriate response-variable relationship, orders of magnitude and mathematical signs of each coefficient resulted for a linear correlation factor of $R^2 = 0.60$ for input variables cholesterol concentration (X_2), mixing time (X_3) and mixing speed (X_4) demonstrated combinations of X_1&X_2, X_1&X_3, X_1&X_4, X_3&X_5 variables had considerably favorable Y_1 due to the desired increase in % entrapment efficiency.

Alternatively, X_2&X_3, X_2&X_4, X_3&X_4, X_1&X_5, X_2&X_5, X_4&X_5 resulted in unfavorable % encapsulation efficiency due to decreased entrapment efficiency. Input variable surfactant concentration (X_1) and addition rate (X_5) possess inverse proportionality with entrapment efficiency. No linear correlations were drawn between responses and factors at ranges used in selected formations.

Table 4. Summary of results of regression analysis for response Y_1.

Quadratic Model	R^2	Adjusted R^2
Response (Y_1) entrapment efficiency	0.600	0.22536

Regression analysis for the entrapment efficiency of the polynomial model was established using the equation shown:

Niosomes entrapment efficiency (Y_1) = $90.12 - 0.56(X_1) + 0.27(X_2) + 0.17(X_3) + 0.36(X_4) - 0.75(X_5) + 0.32(X_1X_2) + 0.30(X_1X_3) - 0.02(X_2X_3) + 0.56(X_1X_4) - 0.03(X_2X_4) - 0.67(X_3X_4) - 0.11(X_1X_5) - 0.12(X_2X_5) + 0.24(X_3X_5) - 0.25(X_4X_5)$

Where X_1 is Span 60 (mg), X_2 is cholesterol (mg), X_3 is mixing speed (RPM), X_4 is mixing time (minutes), and X_5 is addition rate (mL/min).

3.3.1.1. Contour model graph for entrapment efficiency

The two-dimensional (2D) contour plots compare the effects of two independent variables. The interactions between the values of two independent variables that showed no linear correlation, while the remaining three independent variables remained at constant to illustrate their respective response interactions shown in Figure 1 (a-j).

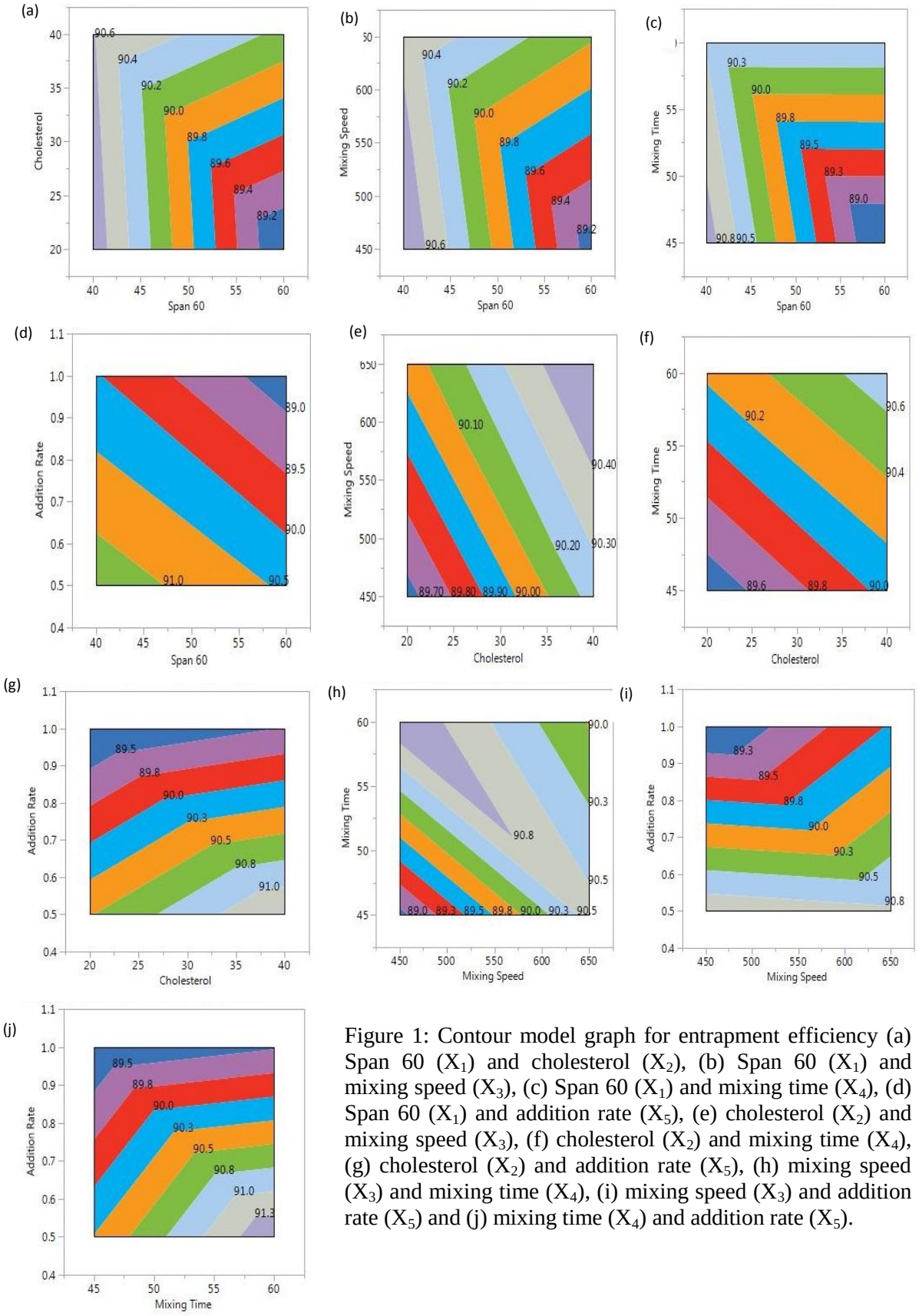

Figure 1: Contour model graph for entrapment efficiency (a) Span 60 (X_1) and cholesterol (X_2), (b) Span 60 (X_1) and mixing speed (X_3), (c) Span 60 (X_1) and mixing time (X_4), (d) Span 60 (X_1) and addition rate (X_5), (e) cholesterol (X_2) and mixing speed (X_3), (f) cholesterol (X_2) and mixing time (X_4), (g) cholesterol (X_2) and addition rate (X_5), (h) mixing speed (X_3) and mixing time (X_4), (i) mixing speed (X_3) and addition rate (X_5) and (j) mixing time (X_4) and addition rate (X_5).

3.3.1.2. Effect of Span 60 (surfactant) concentration on entrapment efficiency

Contour plot analysis showed that in the case of interaction between (a) Span 60 (X_1) and cholesterol (X_2) at other three variables constant, (b) Span 60 (X_1) and mixing speed (X_3) at other three variables constant, (c) Span 60 (X_1) and mixing time (X_4) at other three variables constant, (d) Span 60 (X_1) and addition rate (X_5) at other three variables constant, the response of Span 60 was reasonably partial. With the gradient inclination of Span 60 concentration, the entrapment efficiency was gradually and inversely decreasing. The explanation is related to the compromised polymer availability for the small particles, which decreases flexibility at a higher Span 60 concentration. With low flexibility, the likelihood of membrane irregularities and even vesicle rupture are quite high. A similar trend was also observed and reported in the published literature.[42]

3.3.1.3. Effect of cholesterol concentration on entrapment efficiency

Contour plot analysis showed that in the case of (a) Span 60 (X_1) and cholesterol (X_2) at other three variables constant, (e) cholesterol (X_2) and mixing speed (X_3) at other three variables constant, (f) cholesterol (X_2) and mixing time (X_4) at other three variables constant, (g) cholesterol (X_2) and addition rate (X_5) at other three variables constant, the response of cholesterol was reasonably partial. With the gradient inclination of cholesterol concentration, the entrapment efficiency was increasing gradually, except it shows an inverse trend when increasing Span 60 concentration. Cholesterol is the key ingredient for the niosome vesicle formation. Increasing cholesterol concentration increases membrane rigidity and thus increasing of percentage entrapment efficiency by the formation of less leaky vesicles. These results were found to be consistent with trends published in previous literature.[43]

3.3.1.4. Effect of mixing speed on entrapment efficiency

Contour plot analysis showed in the case of (a) Span 60 (X_1) and mixing speed (X_3) at other three variables constant, (b) cholesterol (X_2) and mixing speed (X_3) at other three variables constant, (c) mixing speed (X_3) and mixing time (X_4) at other three variables constant, (d) mixing speed (X_3) and addition rate (X_5) at other three variables constant, the response of mixing speed variations was observed to be quite arbitrary when evaluated against Span 60 and addition rate. Entrapment efficiency appears to be increasing with gradually increasing mixing speed along with cholesterol. At higher mixing time and lower mixing speed, the entrapment efficiency was also seen to increase. As mixing speed increases gradually, it shows an opposite trend in entrapment efficiency.

3.3.1.5. Effect of mixing time on entrapment efficiency

Contour plot analysis showed in the case of (a) Span 60 (X_1) and mixing time (X_4) at other three variables constant, (b) cholesterol (X_2) and mixing time (X_4) at other three variables constant, (c) mixing speed (X_3) and mixing time (X_4) at other three variables constant, (d) mixing time (X_4) and addition rate (X_5) at other three variables constant, the response of mixing time was quite arbitrary when evaluated against Span 60. Entrapment efficiency shows an upward trend with gradually increasing mixing time along with cholesterol. At lower addition rate, entrapment efficiency is higher and shows gradually increasing trend with increasing mixing time. At higher mixing time and lower mixing speed, entrapment efficiency is seen to increase. As mixing speed increases gradually, it shows a decreasing trend in entrapment efficiency. Overall, it is clear that mixing time has a direct impact on entrapment efficiency. This behavior can be explained as longer mixing time provides adequate hydration time, which shows better dispersibility and helps in providing rigid and less leaky niosomes.

3.3.1.6. Effect of addition rate on entrapment efficiency

Contour plot analysis showed in the case of (a) Span 60 (X_1) and addition rate (X_5) at other three variables constant, (b) cholesterol (X_2) and addition rate (X_5) at other three variables constant, (c) mixing speed (X_3) and addition rate (X_5) at other three variables constant, (d) mixing time (X_4) and addition rate (X_5) at other three variables constant, the response of addition rate is quite constant and shows better entrapment efficiency at slower addition rate regardless of other variables. This behavior can be explained as a slower addition rate, in the end, increase total mixing time, which provides adequate hydration time with better dispersibility and helps in providing rigid and less leaky niosomes.

3.3.1.7. Response surface analysis for entrapment efficiency

Response surface analysis further explained that in all probable cases of interactions, Span 60 (X_1) and cholesterol (X_2) with other three variables constant provided controllable and favorable range of entrapment efficiency to the niosomes. The surface response curve in Figure 2 further justified this conclusion. Based on contour plots and response surface analysis conclusion recommended a specific combination of Span 60 (X_1) and cholesterol (X_2) while keeping the other three variables constant to achieve entrapment efficiency within a desirable range.

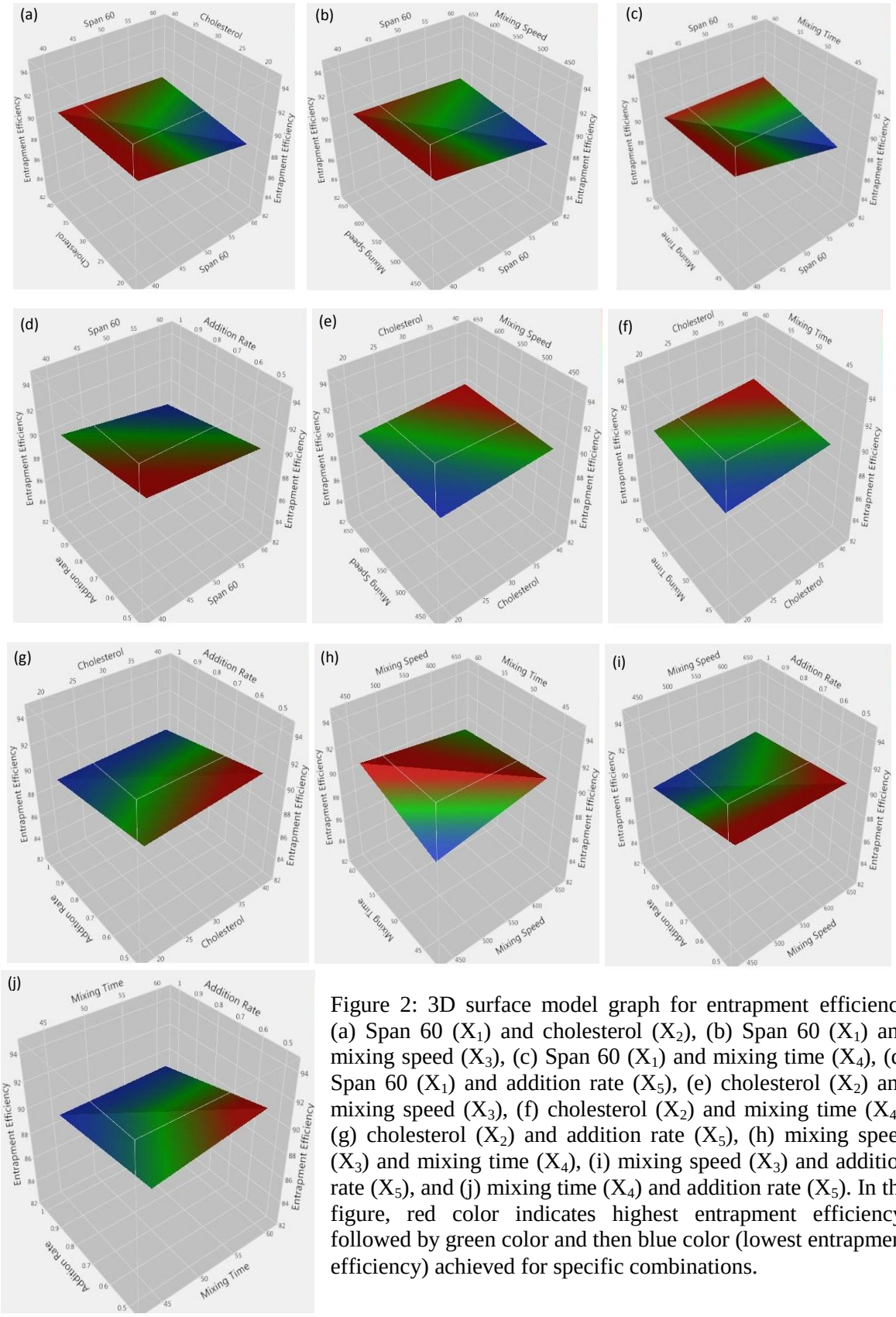

Figure 2: 3D surface model graph for entrapment efficiency (a) Span 60 (X_1) and cholesterol (X_2), (b) Span 60 (X_1) and mixing speed (X_3), (c) Span 60 (X_1) and mixing time (X_4), (d) Span 60 (X_1) and addition rate (X_5), (e) cholesterol (X_2) and mixing speed (X_3), (f) cholesterol (X_2) and mixing time (X_4), (g) cholesterol (X_2) and addition rate (X_5), (h) mixing speed (X_3) and mixing time (X_4), (i) mixing speed (X_3) and addition rate (X_5), and (j) mixing time (X_4) and addition rate (X_5). In the figure, red color indicates highest entrapment efficiency, followed by green color and then blue color (lowest entrapment efficiency) achieved for specific combinations.

3.3.2. Response 2 (Y_2): effect of formulation variables on particle size

Analyzing this response for particle size did not require further plot transformation. A best fit model represented an R^2 value is 0.59, which represented that all of the CMAs & CPPs had a significant impact on noisome particle size. The allusion was drawn from the magnitude and mathematical sign of each coefficient.

The regression equation explains that the resulting impact of surfactant concentration (X_1), cholesterol concentration (X_2), mixing time (X_3), mixing speed (X_4) and addition rate (X_5) as they all demonstrated an inverse relationship with niosome particle size.

In some cases, the relationship between responses and factors were not always linear and suggested that interactions existed between variables. Favorable interactions for particle size were found using X_1&X_2, X_2&X_3, X_2&X_4, X_3&X_4, X_1&X_5, X_3&X_5, X_4&X_5 combination that decreased particle size, while X_1&X_3, X_1 &X_4, X_2&X_5 increased particle size of Y_2 response.

Table 5: Summary of results of regression analysis for response Y_2.

Quadratic Model	R^2	Adjusted R^2
Response (Y_2) particle size	0.591	0.209481

After a regression analysis for the particle size, the polynomial model established as described here:

Niosomes particle size (Y_2) = 671.50 – 42.16(X_1) – 65.77(X_2) – 124.98(X_3) – 7.95(X_4) – 27.59(X_5) – 93.02(X_1X_2) + 7.98(X_1X_3) – 25.62(X_2X_3) + 37.77(X_1X_4) – 64.99(X_2X_4) – 18.92(X_3X_4) – 28.79(X_1X_5) + 31.24(X_2X_5) – 14.17(X_3X_5) – 49.18(X_4X_5)

Where X_1 is Span 60 (mg), X_2 is cholesterol (mg), X_3 is mixing speed (rpm), X_4 is mixing time (min) and X_5 is addition rate (mL/min).

3.3.2.1. Contour model graph for niosomal particle size

The interaction between the two independent variables remain constant while the other three independent variables is shown in Figure 3 (a-j).

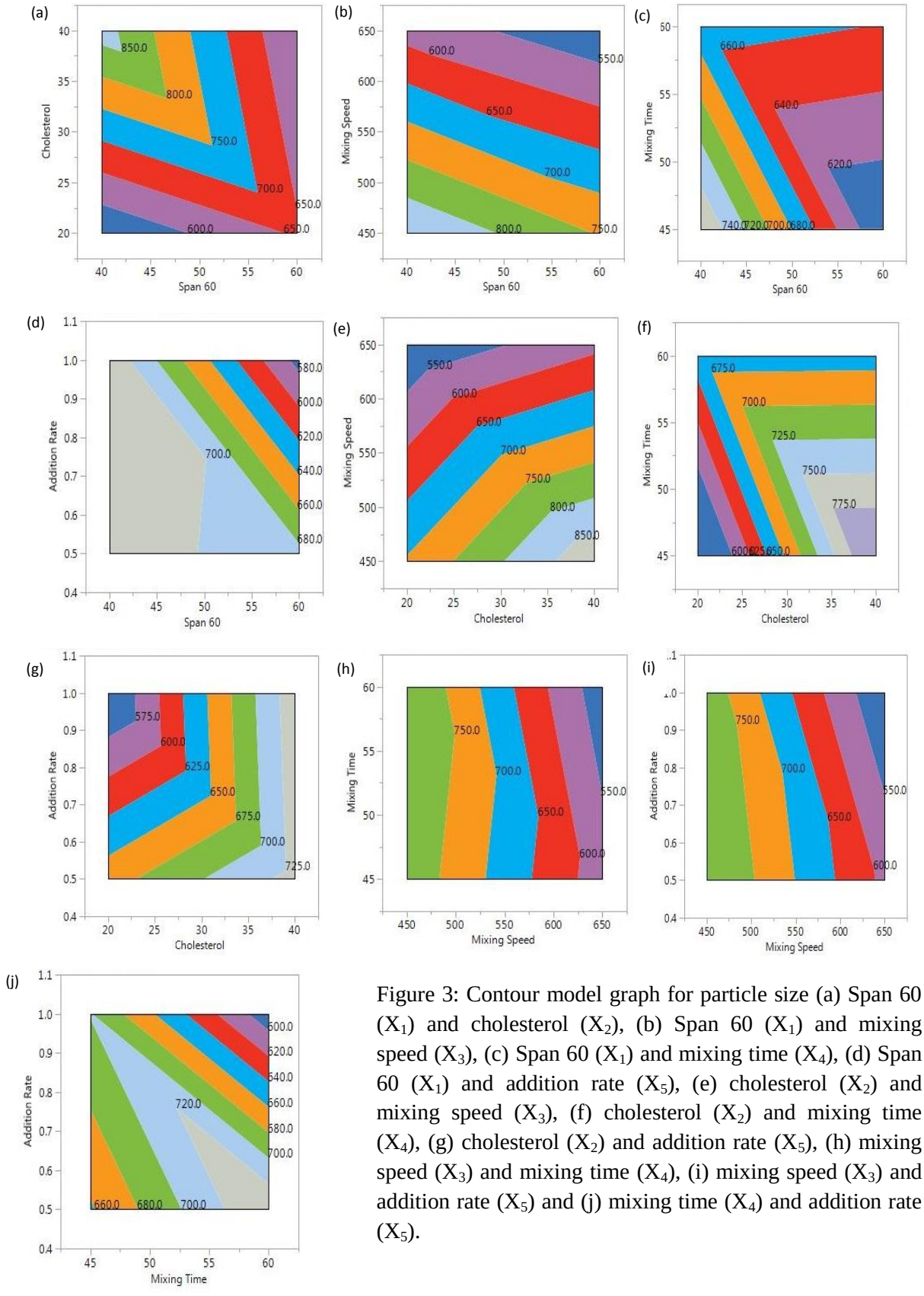

Figure 3: Contour model graph for particle size (a) Span 60 (X_1) and cholesterol (X_2), (b) Span 60 (X_1) and mixing speed (X_3), (c) Span 60 (X_1) and mixing time (X_4), (d) Span 60 (X_1) and addition rate (X_5), (e) cholesterol (X_2) and mixing speed (X_3), (f) cholesterol (X_2) and mixing time (X_4), (g) cholesterol (X_2) and addition rate (X_5), (h) mixing speed (X_3) and mixing time (X_4), (i) mixing speed (X_3) and addition rate (X_5) and (j) mixing time (X_4) and addition rate (X_5).

3.3.2.2. Effect of Span 60 (surfactant) concentration on niosomal particle size

Contour plot analysis showed in the case of (a) Span 60 (X_1) and cholesterol (X_2) at other three variables constant, (b) Span 60 (X_1) and mixing speed (X_3) at other three variables constant, (c) Span 60 (X_1) and mixing time (X_4) at other three variables constant, (d) Span 60 (X_1) and addition rate (X_5) at other three variables constant, the response of Span 60 concentration is quite arbitrary. Where it is trending proportionally as cholesterol concentration, mixing speed, mixing time, and addition rate cases, which shows decreasing particle size with increasing Span 60 concentration. This can be explained as high surfactant concentration decreases surface tension and stabilizes newly developed vesicle surfaces during the manufacturing and produce smaller particles. The observed change in particle size with the change in surfactant concentration was seen to be verified with the findings reported in previous literature.[44]

3.3.2.3. Effect of cholesterol concentration on niosomal particle size

Contour plot analysis showed that in the case of (a) Span 60 (X_1) and cholesterol (X_2) at other three variables constant, (e) cholesterol (X_2) and mixing speed (X_3) at other three variables constant, (f) cholesterol (X_2) and mixing time (X_4) at other three variables constant, (g) cholesterol (X_2) and addition rate (X_5) at other three variables constant, the response of cholesterol was reasonably consistent. In the presence of other variables with the gradient inclination of cholesterol concentration, the particle size was seen to increase gradually. It can be concluded that cholesterol is one of the critical ingredients for the niosome formation. The observed increase in mean vesicle size of desoximetasone niosomes with the addition of cholesterol was seen to conform with the findings reported in prior literature.[43,45]

3.3.2.4. Effect of mixing speed on niosomal particle size

Contour plot analysis showed in the case of (b) Span 60 (X_1) and mixing speed (X_3) at other three variables constant, (e) cholesterol (X_2) and mixing speed (X_3) at other three variables constant, (h) mixing speed (X_3) and mixing time (X_4) at other three variables constant, (i) mixing speed (X_3) and addition rate (X_5) at other three variables constant, the response of mixing speed was reasonably consistent. With the gradient inclination of mixing speed, a gradual decrease in the particle size of the niosomes was observed. These results are supported by previous works that reported the dependence of vesicle size on the method of preparation, bilayer composition, and bio-component concentration.[46,47]

3.3.2.5. Effect of mixing time on niosomal particle size

Contour plot analysis showed in the case of (c) Span 60 (X_1) and mixing time (X_4) at other three variables constant, (f) cholesterol (X_2) and mixing time (X_4) at other three variables constant, (h) mixing speed (X_3) and mixing time (X_4) at other three variables constant, (j) mixing time (X_4) and addition rate (X_5) at other three variables constant, the response of mixing time was quite arbitrary. The reaction of mixing time is constant with minimum impact when it was evaluated against mixing speed. When assessed against the addition rate, it was seen that lower mixing time/addition rate or higher mixing time/addition rate combination is required to achieve desirable smaller particle size. Regardless of other variables, and the increase in mixing time shows a decrease in particle size. This behavior can be explained as longer mixing time provides adequate hydration time and shows better dispersibility, which can further provide smaller and uniform niosomes. Similar findings have been observed in previous published work.[48]

3.3.2.6. Effect of addition rate on niosomal particle size

Contour plot analysis showed in the case of (d) Span 60 (X_1) and addition rate (X_5) at other three variables constant, (g) cholesterol (X_2) and addition rate (X_5) at other three variables constant, (i) mixing speed (X_3) and addition rate (X_5) at other three variables constant, (j) mixing time (X_4) and addition rate (X_5) at other three variables constant, the response of addition rate is quite constant. Particle size is comparatively constant when it is evaluated against Span 60, cholesterol, and mixing speed and changes gradually with changes in variables other than the addition rate. This behavior indicates that other variables have a dominant impact on niosomes particle size as compared to the addition rate. When it is evaluated against mixing time, combinations of lower addition rate/mixing time or higher addition rate/mixing time is seen to be required to achieve desirable smaller particle size.

3.3.2.7. Response surface analysis for niosomal particle size

Response surface analysis further explained that in all probable cases of interactions, Span 60 (X_1) and cholesterol (X_2) at other three variables constant was providing a controllable and favorable range of particle size. The surface response curve in Figure 4 further justified these conclusions.

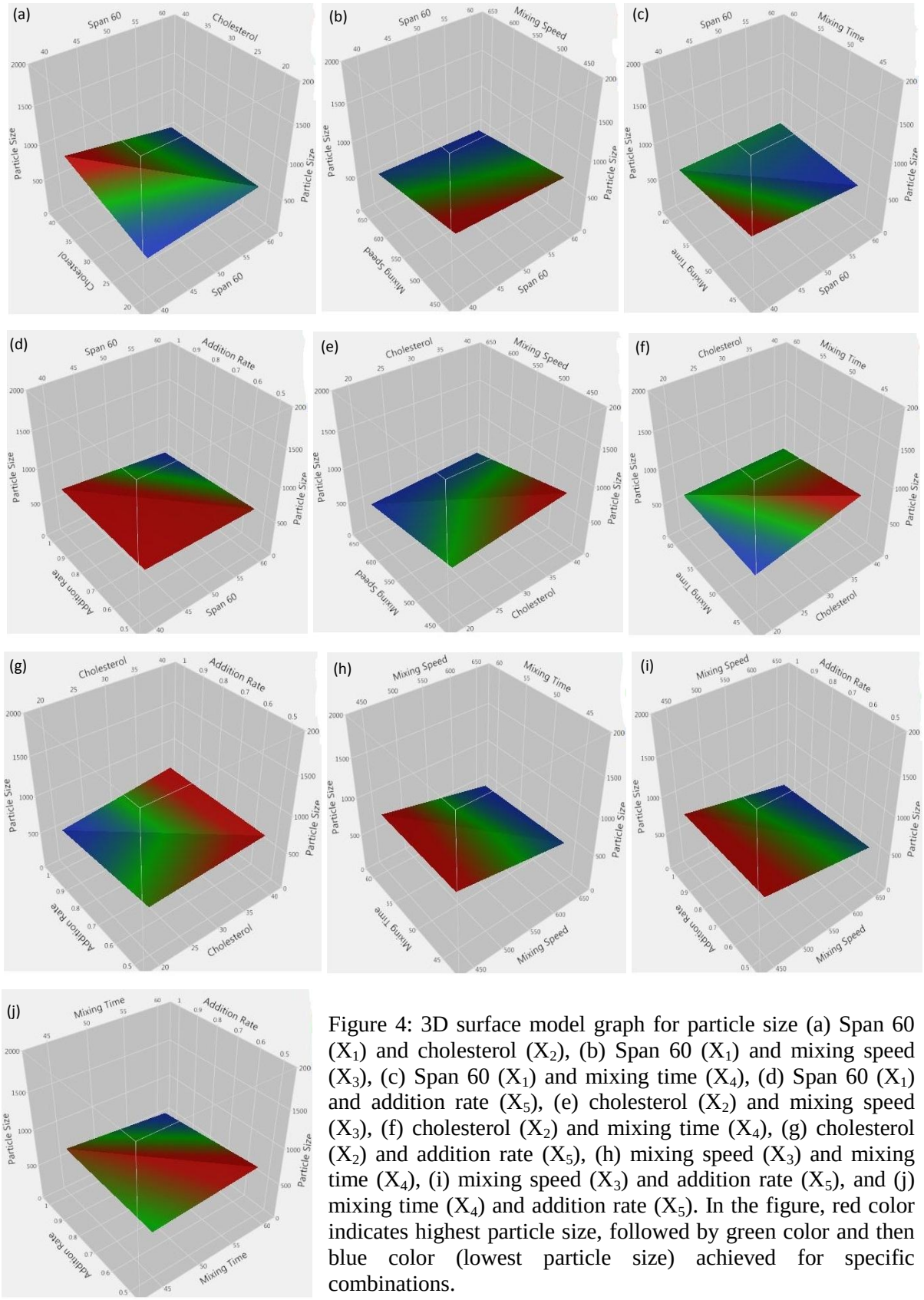

Figure 4: 3D surface model graph for particle size (a) Span 60 (X_1) and cholesterol (X_2), (b) Span 60 (X_1) and mixing speed (X_3), (c) Span 60 (X_1) and mixing time (X_4), (d) Span 60 (X_1) and addition rate (X_5), (e) cholesterol (X_2) and mixing speed (X_3), (f) cholesterol (X_2) and mixing time (X_4), (g) cholesterol (X_2) and addition rate (X_5), (h) mixing speed (X_3) and mixing time (X_4), (i) mixing speed (X_3) and addition rate (X_5), and (j) mixing time (X_4) and addition rate (X_5). In the figure, red color indicates highest particle size, followed by green color and then blue color (lowest particle size) achieved for specific combinations.

Based on contour plots and response surface analysis, specific combinations of Span 60 (X_1) and cholesterol (X_2) keeping the other three variables constant can be concluded important to

achieve a favorable range of maximum entrapment efficiency and minimum particle size of the niosomes. A further selection is based on the validation checkpoints generated by the software.

3.4. Confirmation and validation of DOE

Validating an experimental design model consisted of two checkpoint niosome formulations (DND-62 and DND-63) to accurately predict entrapment efficiency and particle size using the profile predictor model provided by JMP® software. Niosome formulations were manufactured to comparatively study entrapment efficiency and particle size, as provided in Table 6 and Table 7, respectively.

Table 6: Composition of checkpoint formulations, expected and observed value for response variable of niosomes entrapment efficiency (N = 3, mean ± SD).

	Variable parameters					Entrapment efficiency	
Batch Detail	**Span 60 (mg)**	**Cholesterol (mg)**	**Mixing time (min)**	**Mixing speed (rpm)**	**Addition rate (mL/min)**	**Expected value (%)**	**Observed value ± S.D (%)**
DND-62	40	20	50	650	0.5	91.11	90.19 ± 0.02
DND-63	40	40	60	500	1.0	89.66	87.27 ± 0.01

Table 7: Composition of checkpoint formulations, expected and observed value for response variable of niosomes particle size (N = 3, mean ± SD).

	Variable parameters					Particle size	
Batch Detail	**Span 60 (mg)**	**Cholesterol (mg)**	**Mixing time (min)**	**Mixing speed (rpm)**	**Addition rate (mL/min)**	**Expected value (nm)**	**Observed value ± S.D (nm)**
DND-62	40	20	50	650	0.5	475.20	449.40 ± 29.2
DND-63	40	40	60	500	1.0	840.85	813.43 ± 173.8

No significant differences between the observed and the expected values were observed using this model, which concluded the model accurately predicted the entrapment efficiency & particle size using the experimental design mentioned. Formulation DND-62 resulted in significantly higher entrapment efficiency and smaller particle size compared with the formulation DND-63.

DND-62 was selected for use in a further study to optimize desoximetasone-loaded niosomes based on the desired criteria of niosome size and maximum entrapment efficiency. Formulation composition containing – drug: surfactant: cholesterol (1:2:1), diethyl ether: methanol (75:25), external phase temperature (65°C), external phase volume: internal phase

volume (2:1), mixing speed (650 rpm), mixing time (50 min) and addition rate (0.5 mL/min) successfully developed a final noisome formulation with optimal particle size and drug entrapment efficiency.

3.5. Characterization of optimized niosomes

3.5.1. Entrapment efficiency of niosome

Drug entrapment of the optimized niosomes loaded with desoximetasone was determined with the validated HPLC method, and entrapment efficiency was found to be 90.19 ± 0.02 %, which describes an appreciable drug loading in niosomes vesicles.

3.5.2. Niosome size and distribution

The size of the optimized niosomes was found to be 449.40 ± 29.2 nm, with a polydispersity index (PDI) of 0.272 ± 0.03.

3.5.3. Zeta potential

Zeta potential of the optimized niosome formulation DND-62 was found to be -73.50 ± 0.87 mV. Favorable stability of these vesicles associated with higher absolute values ± 30 mV mitigate stability risk while using surfactants.[49] Higher zeta potential values typically result in an increased due to repulsion charges, which prevent particle aggregation.

4. CONCLUSION

Optimization of niosomes for use in topical applications requires a comprehensive understanding of numerous variables that may even be interdependent with each other. The current work demonstrated the effective use of a systematic full factorial design methodology to successfully predict an ideal niosome vesicles containing desoximetasone for topical applications. Formulations obtained for relevant performance efficacy characteristics using *in vitro*, *ex vivo* and *in vivo* testing techniques. The results show how niosomes were modified to achieve an effective drug delivery profile selecting appropriate parameters for Span 60, cholesterol, mixing time, mixing speed, and addition rate. The entrapment efficiency and particle size of the optimized niosome formulation (DND-62) was accurately predicted using JMP® software. The methods described to create desoximetasone-loaded niosomes may have the potential to effectively optimize drug-vehicles in other formulations for various drug delivery applications.

Funding

Funding for this study was provided by the Center for Dermal Research (CDR) at Rutgers, The State University of New Jersey, Piscataway NJ 08854.

Conflict of interest

The authors declare no conflict of interest.

REFERENCES

1. Roberts M, Mohammed Y, Pastore M, Namjoshi S, Yousef S, Alinaghi A, et al. Topical and cutaneous delivery using nanosystems. Journal of controlled release, 2017; 247: 86-105.
2. Bouyer E, Mekhloufi G, Rosilio V, Grossiord J-L, Agnely F. Proteins, polysaccharides, and their complexes used as stabilizers for emulsions: alternatives to synthetic surfactants in the pharmaceutical field? International journal of pharmaceutics., 2012; 436(1-2): 359-78.
3. Simões A, Veiga F, Vitorino C, Figueiras A. A tutorial for developing a topical cream formulation based on the quality by design approach. Journal of pharmaceutical sciences, 2018; 107(10): 2653-62.
4. Waldman AR, Ahluwalia J, Udkoff J, Borok JF, Eichenfield LF. Atopic Dermatitis. Pediatrics in Review., 2018; 39(4): 180-93.
5. Boguniewicz M LD. Atopic dermatitis in: Middleton's allergy: principles and practice. 8th ed: Elsevier Inc., 2014; 540-64.
6. Rattner H. The status of corticosteroid therapy in dermatology. California medicine, 1955; 83(5): 331.
7. Robertson DB, Maibach HI. Topical corticosteroids. International journal of dermatology, 1982; 21(2): 59-67.
8. Kimball AB, Gladman D, Gelfand JM, Gordon K, Horn EJ, Korman NJ, et al. National Psoriasis Foundation clinical consensus on psoriasis comorbidities and recommendations for screening. Journal of the American Academy of Dermatology, 2008; 58(6): 1031-42.
9. Enamandram M, Kimball AB. Psoriasis epidemiology: the interplay of genes and the environment. Journal of Investigative Dermatology.,2013; 133(2): 287-9.
10. Lagos B, Maibach H. Frequency of application of topical corticosteroids: an overview. The British journal of dermatology., 1998; 139(5): 763-6.

11. Wolkerstorfer A, Strobos MA, Glazenburg EJ, Mulder PG, Oranje AP. Fluticasone propionate 0.05% cream once daily versus clobetasone butyrate 0.05% cream twice daily in children with atopic dermatitis. Journal of the American Academy of Dermatology, 1998; 39(2): 226-31.
12. Patel H, Parikh VP. An overview of osmotic drug delivery system: an update review. International Journal of Bioassays., 2017; 6(7): 5426-36.
13. Aubert-Wastiaux H, Moret L, Le Rhun A, Fontenoy A, Nguyen J, Leux C, et al. Topical corticosteroid phobia in atopic dermatitis: a study of its nature, origins and frequency. British journal of dermatology., 2011; 165(4): 808-14.
14. Cornell R, Stoughton R. Six-month controlled study of effect of desoximetasone and betamethasone 17-valerate on the pituitary-adrenal axis. British Journal of dermatology, 1981; 105(1): 91-5.
15. Savin R. Desoximetasone--a new topical corticosteroid: short-and long-term experiences. Cutis., 1978; 21(3): 403-7.
16. Lundell E. A double blind trial of a new topical steroid formulation containing desoximetasone against fluocinolonacetonid cream. Zeitschrift fur Hautkrankheiten, 1975; 17-9.
17. Cornell R. Clinical trials of topical corticosteroids in psoriasis: correlations with the vasoconstrictor assay. International journal of dermatology., 1992; 31: 38-40.
18. Borelli C, Gassmueller J, Fluhr J, Nietsch K, Schinzel S, Korting HC. Activity of different desoximetasone preparations compared to other topical corticosteroids in the vasoconstriction assay. Skin pharmacology and physiology., 2008; 21(3): 181-7.
19. Chen S, Hanning S, Falconer J, Locke M, Wen J. Recent advances in non-ionic surfactant vesicles (niosomes): Fabrication, characterization, pharmaceutical and cosmetic applications. European Journal of Pharmaceutics and Biopharmaceutics., 2019; 144: 18-39.
20. Ag Seleci D, Seleci M, Walter J-G, Stahl F, Scheper T. Niosomes as Nanoparticular Drug Carriers: Fundamentals and Recent Applications. Journal of Nanomaterials., 2016; 2016: 13.
21. Uchegbu IF, Vyas SP. Non-ionic surfactant based vesicles (niosomes) in drug delivery. International journal of pharmaceutics., 1998; 172(1-2): 33-70.

22. Handjani-Vila R, Ribier A, Rondot B, Vanlerberghie G. Dispersions of lamellar phases of non-ionic lipids in cosmetic products. International journal of cosmetic Science, 1979; 1(5): 303-14.
23. Kazi KM, Mandal AS, Biswas N, Guha A, Chatterjee S, Behera M, et al. Niosome: a future of targeted drug delivery systems. Journal of advanced pharmaceutical technology & research., 2010; 1(4): 374.
24. El-Ridy MS, Badawi AA, Safar MM, Mohsen AM. Niosomes as a novel pharmaceutical formulation encapsulating the hepatoprotective drug silymarin. Int J Pharm Pharm Sci., 2012; 4(1): 549-59.
25. Frey DD, Engelhardt F, Greitzer EM. A role for" one-factor-at-a-time" experimentation in parameter design. Research in Engineering Design., 2003; 14(2): 65-74.
26. Hibbert DB. Experimental design in chromatography: a tutorial review. Journal of chromatography B., 2012; 910: 2-13.
27. Teja S, Mothilal M, Damodharan N, Jaison D. Screening and optimization of valacyclovir niosomes by design of experiments. Int J App Pharm, 2017; 10(1): 79. 2018-85.
28. Ye C, Liu J, Ren F, Okafo N. Design of experiment and data analysis by JMP®(SAS institute) in analytical method validation. Journal of pharmaceutical and biomedical analysis., 2000; 23(2-3): 581-9.
29. Srinivasulu K, Naidu MN, Rajasekhar K, Veerender M, Suryanarayana MV. Development and validation of a stability indicating LC method for the assay and related substances determination of a proteasome inhibitor bortezomib. Chromatography Research International., 2012.
30. Jain S. Quality by design (QBD): a comprehensive understanding of implementation and challenges in pharmaceuticals development. Int J Pharm Pharm Sci., 2014; 6: 29-35.
31. Zhang L, Mao S. Application of quality by design in the current drug development. Asian journal of pharmaceutical sciences., 2017; 12(1): 1-8.
32. Lawrence XY. Pharmaceutical quality by design: product and process development, understanding, and control. Pharmaceutical research., 2008; 25(4): 781-91.
33. Lawrence XY, Amidon G, Khan MA, Hoag SW, Polli J, Raju G, et al. Understanding pharmaceutical quality by design. The AAPS journal., 2014; 16(4): 771-83.
34. Khanolkar A, Thorat V, Raut P, Samanta G. Application of Quality by Design: development to manufacturing of diclofenac sodium topical gel. AAPS PharmSciTech., 2017; 18(7): 2754-63.
35. Q9 quality risk management. ICH, Guidance for industry., 2005.

36. Q10 pharmaceutical quality system. ICH, Guidance for industry., 2008.
37. Q8(R2) pharmaceutical develop-ment ICH, Guidance for industry, 2009.
38. Shah P, Goodyear B, Haq A, Puri V, Michniak-Kohn B. Evaluations of Quality by Design (QbD) Elements Impact for Developing Niosomes as a Promising Topical Drug Delivery Platform. Pharmaceutics., 2020; 12(3): 246.
39. Goyal G, Garg T, Malik B, Chauhan G, Rath G, Goyal AK. Development and characterization of niosomal gel for topical delivery of benzoyl peroxide. Drug delivery., 2015; 22(8): 1027-42.
40. Ozer A, Hincal A, Bouwstra J. A novel drug delivery system-nonionic surfactant vesicles, 1991; 37: 75-9.
41. Jivrani SD, Patel VK. Formulation, Development And Evaluation Of Niosomal Drug Delivery System For Clindamycin Phosphate. Pharma Science Monitor., 2014; 5.
42. Shah C, Shah D. Design and optimization of fluconazole microsponges containing ethyl cellulose for topical delivery system using quality by design approach. Pharma Science Monitor., 2014; 5(3): 95-133.
43. Bendas ER, Abdullah H, El-Komy MH, Kassem MA. Hydroxychloroquine niosomes: a new trend in topical management of oral lichen planus. International journal of pharmaceutics., 2013; 458(2): 287-95.
44. Zirak MB, Pezeshki A. Effect of surfactant concentration on the particle size, stability and potential zeta of beta carotene nano lipid carrier. Int J Curr Microbiol Appl Sci., 2015; 4(9): 924-32.
45. Pardakhty A, Varshosaz J, Rouholamini A. In vitro study of polyoxyethylene alkyl ether niosomes for delivery of insulin. International journal of pharmaceutics., 2007; 328(2): 130-41.
46. Manconi M, Sinico C, Valenti D, Loy G, Fadda AM. Niosomes as carriers for tretinoin. I. Preparation and properties. International journal of pharmaceutics., 2002; 234(1-2): 237-48.
47. Pando D, Gutiérrez G, Coca J, Pazos C. Preparation and characterization of niosomes containing resveratrol. Journal of Food Engineering., 2013;117(2): 227-34.
48. Yeo LK, Chaw CS, Elkordy AA. The Effects of Hydration Parameters and Co-Surfactants on Methylene Blue-Loaded Niosomes Prepared by the Thin Film Hydration Method. Pharmaceuticals., 2019; 12(2): 46.

49. Sezgin-Bayindir Z, Antep MN, Yuksel N. Development and characterization of mixed niosomes for oral delivery using candesartan cilexetil as a model poorly water-soluble drug. AAPS PharmSciTech., 2015; 16(1): 108-17.